

## Materials and Methods

### Whole cell electrophysiology

The codon-optimized cDNAs of wild-type Na<sub>v</sub>1.7 (Na<sub>v</sub>1.7-WT, UniProt: Q15858) and Na<sub>v</sub>1.7-M9 (L866F, T870M, A874F, V947F, M952F, V953F, V1438I, V1439F, and G1454C) were synthesized (BGI Geneland Scientific Co.,Ltd) and subcloned into the pEG BacMam vector with twin Strep-tag and FLAG tag in tandem at the amino terminus (1). Na<sub>v</sub>1.7-M11 was generated by introducing two addition mutations, E156K and G779R, to Na<sub>v</sub>1.7-M9 using a standard two-step PCR-based strategy. All plasmids were validated by DNA sequencing and prepared with a HiPure Plasmid EF Mini Kit (Magen). For whole-cell patch-clamp recordings, HEK293T cells (Invitrogen) were cultured in Dulbecco's Modified Eagle Medium (DMEM, BI) supplemented with 4.5 mg/mL glucose and 10% (v/v) fetal bovine serum (FBS, BI). Cells for recordings were plated onto glass coverslips and transiently co-transfected with the expression plasmid for Na<sub>v</sub>1.7 variants and an eGFP-encoding plasmid using lipofectamine 2000 (Invitrogen). Cells with green fluorescence were selected for patch-clamp recording 18–36 h after transfection. All experiments were performed at room temperature. No further authentication was performed for the commercially available cell line. *Mycoplasma* contamination was not tested.

The whole-cell Na<sup>+</sup> currents were recorded using an EPC10-USB amplifier with Patchmaster software v2\*90.2 (HEKA Elektronik), filtered at 3 kHz (low-pass Bessel filter) and sampled at 50 kHz. The borosilicate pipettes (Sutter Instrument) had a resistance of 2-4 MΩ and the electrodes were filled with the internal solution composed of (in mM) 105 CsF, 40 CsCl, 10 NaCl, 10 EGTA, 10 Hepes, pH 7.4 with CsOH for WT

and M9. The bath solutions contained (in mM): 140 NaCl, 4 KCl, 10 Hepes, 10 D-glucose, 1 MgCl<sub>2</sub>, 1.5 CaCl<sub>2</sub>, pH 7.4 with NaOH for WT and M9. To analyze M11, which showed positively shifted activation curve from preliminary recordings, solutions were designed to give a reversal potential of 0 mV for Na<sup>+</sup>, with the internal solutions (in mM): 105 CsF, 35 NaCl, 10 EGTA, 10 Hepes, pH 7.4 with CsOH, and bath solutions (in mM): 105 NMDG-Cl, 35 NaCl, 2 MgCl<sub>2</sub>, 2 CaCl<sub>2</sub>, 10 Hepes, pH 7.4 with NMDG<sup>+</sup>. Data were analyzed using Origin (OriginLab) and GraphPad Prism (GraphPad Software).

The voltage dependence of ion current (I-V) was analyzed using a protocol consisting of steps from a holding potential of -120 mV for WT/M9 and -150 mV for M11 for 200 ms to voltages ranging from -90 to 80 mV for WT/M9 and from -50 mV to 180 mV for M11 for 50 ms in 5 mV increment. The linear component of leaky currents and capacitive transients were subtracted using the P/4 procedure.

In the activation calculation, we used the equation,  $G = I / (V - V_r)$ , where  $V_r$  (the reversal potential) represents the voltage at which the current is zero. As the I-V curves of M11 contain only outward current, the  $V_r$  for M11 was determined from the tail currents at peak activation. For the activation curves, conductance (G) was normalized and plotted against the voltage from -90 mV to 20 mV for WT, from -90 mV to 60 mV for M9, and from 0 mV to 180 mV for M11.

For voltage dependence of inactivation, cells were clamped at a holding potential of -90 mV, and were applied to step prepulses from -120 mV to 20 mV for WT/M9 and from -150 mV to 40 mV for M11 for 1000 ms with an increment of 5 or 10 mV. Then, the Na<sup>+</sup> currents were recorded at the test pulse of 0 mV for WT, 10 mV for M9, and 150 mV for

M11 for 50 ms. The peak currents under the test pulses were normalized and plotted against the prepulse voltage.

Activation and inactivation curves were fit to a Boltzmann function to obtain  $V_{1/2}$  and slope values. Time course of inactivation data from the peak current at 0 mV/10 mV/150mV was fitted with a single exponential equation:  $y = A1 \exp(-x/\tau_{\text{inac}}) + y0$ , where A1 was the relative fraction of current inactivation,  $\tau_{\text{inac}}$  was the time constant, x was the time, and y0 was the amplitude of the steady-state component. For closed-state inactivation, cells were held at a potential of -120 mV for WT/M9 and -150 mV for M11, and then were prepulsed to -70 mV or -50 mV for increasing durations (from 0.6 ms to 1350 ms) before stepped to 0 mV for WT, 10 mV for M9, and 150 mV for M11 for 50 ms to determine the fraction of current inactivated during the prepulse. Entry into closed-state inactivation was obtained by fitting a single exponential decay equation.

All data points are presented as mean  $\pm$  SEM and n is the number of experimental cells from which recordings were obtained. Statistical significance was assessed using one-way ANOVA analysis and extra sum-of-squares F test.

### **Recombinant co-expression and protein purification**

Na<sub>v</sub>1.7-M11 was co-expressed with the auxiliary subunits  $\beta$ 1 and  $\beta$ 2 following an identical protocol as reported (2). For one batch of sample preparation, 40 L transfected cells were harvested by centrifugation at 800 g and resuspended in the lysis buffer containing 25 mM Tris (pH 7.5) and 150 mM NaCl. The suspension was supplemented with protease inhibitors containing 2 mM phenylmethylsulfonyl fluoride (PMSF, VWR), aprotinin (6.5  $\mu$ g/mL, MCE), pepstatin (3.5  $\mu$ g/mL, Sigma), and leupeptin (25  $\mu$ g/mL,

Sigma). After sonication, the cell lysate was incubated with 1% (w/v) n-dodecyl- $\beta$ -D-maltopyranoside (DDM, Anatrace) and 0.1% (w/v) cholesteryl hemisuccinate Tris salt (CHS, Anatrace) at 4 °C for 3 h. Then the solution was ultra-centrifuged at 200,000 g for 30 min, and the supernatant was applied to anti-Flag M2 affinity gel (Sigma) at 4 °C. After flowthrough by gravity, the resin was rinsed four times with the wash buffer (W buffer) that contains 25 mM Tris (pH 7.5), 150 mM NaCl, 0.06% glyco-diosgenin (GDN, Anatrace), and protease inhibitors. The target proteins were eluted with the W buffer plus 200  $\mu$ g/mL FLAG peptide (Sigma). The eluent was then applied to Strep-Tactin Sepharose (IBA), and the wash and elution protocol was the same as for the first-step affinity purification except that 2.5 mM D-desthiobiotin (IBA) was added to the W buffer for elution. The eluent was concentrated using a 100-kDa cut-off Centricon (Millipore) and further purified through Superose-6 column (GE Healthcare) that was pre-equilibrated with the W buffer. The peak fractions were pooled and concentrated to approximately 1 mg/mL for cryo-EM analysis.

### **Cryo-EM data acquisition**

Aliquots of 3.5  $\mu$ L freshly purified protein were placed on glow-discharged holey carbon grids (Quantifoil Au 300 mesh, R1.2/1.3). Grids were blotted for 3.0 s and flash-frozen in liquid ethane cooled by liquid nitrogen with Vitrobot Mark IV (Thermo Fisher). Prepared grids were subsequently transferred to a Titan Krios electron microscopy (Thermo Fisher) operated at 300 kV and equipped with Gatan K3 detector and GIF Quantum energy filter with a slit width of 20 eV. A total of 7352 movie stacks were automatically collected using AutoEMation (3) with a preset defocus range from -1.8  $\mu$ m to -1.5  $\mu$ m in

super-resolution mode at a nominal magnification of 81,000 X. Each stack was exposed for 2.56 s with 0.08 s per frame, resulting in 32 frames per stack. The total dose rate was  $50 \text{ e}^-/\text{\AA}^2$  for each stack. The stacks were motion-corrected with MotionCor2 (4) and binned 2 folds, resulting in a pixel size of 1.08  $\text{\AA}/\text{pixel}$ . Meanwhile, dose weighting was performed (5). The defocus values were estimated with Gctf (6).

### **Image processing**

A diagram for the data processing is presented in *SI Appendix*, Fig. S3. A total of 3,256,316 particles were automatically picked using Gauotomatch. After 2D classification, a total of 1,331,138 good particles were selected for non-uniform refinement in cryoSPARC (7). For each of the last several iterations of the non-uniform refinement, the particle.cs files were converted into RELION (8-10) data.star files using the pyem package (11). A local angular search 3D classification was performed for each .star file with K set to 4-6. In total 912,322 non-redundant particles were selected from the local angular search 3D classification and subjected to the auto-refinement procedure in RELION-3.1, resulting in a final reconstruction at 2.8  $\text{\AA}$  overall resolution. At this stage of the data processing, the density for VSD<sub>I</sub> was poor, exhibiting local resolutions of 8-10  $\text{\AA}$ . To improve the local EM density at this region, we attempted to further classify the remaining particles into different conformational states following the procedure below.

First, the data star from the auto-refinement procedure was fed into the SGD initial model generation procedure of RELION-3.1 (K=1), which was initiated from random initial seeds and terminated after only a few iterations (typically between 3 and 10). Second, the

reference map of each iteration before termination was substituted with the 2.8 Å overall refined EM-density, and the SGD process was then resumed using the optimiser star file generated by RELION. Through this procedure, we attempted to explore the high dimensional manifold that was close to the consensus refinement result using a batch-based step-wise model update routine. Third, the updated EM-map after different SGD update epochs was fed into a Principle Component Analysis (PCA) script to look for large variations within the population. The solved Principle Components were then added to the consensus refinement result after proper scaling of the eigenvector solved from PCA. The used linear coefficients were sampled in the observed range using a fixed interval. Using one eigenvector solved from PCA, 10 different initial models were generated from the consensus refinement result. Finally, the 10 different initial models were used as seeds for the maximum likelihood-based 3D-classification procedure in RELION-3.1, resolving VSD<sub>I</sub> in different conformations.

Upon identification of two conformational states, particles belonging to these individual classes were separated and imported into cryoSPARC, wherein local refinement of these two classes yielded reconstructions at 2.7 Å (class I) and 2.8 Å (class II) resolutions out of 249,473 and 394,163 particles, respectively. The local resolution for VSD<sub>I</sub> was sufficient for model building and side chain assignment (Fig.1D and E, *SI Appendix*, Fig. S3).

### **Model building and structure refinement**

Model building was based on the 2.7 Å and 2.8 Å maps. The coordinates of WT Na<sub>v</sub>1.7-β1-β2 (PDB accession number: 7W9K) were fitted into the EM maps with manual

adjustment in CHIMERA (12). Every residue in the models, with eleven residues mutated, was manually checked and adjusted in COOT (13). The final models contain 1541 and 1529 residues for class I and class II, respectively, and each with 11 sugar moieties and 31 lipid molecules. The intracellular I-II linker (residues 428-725), II-III linker (residues 1015-1174), and the C-terminal sequences after Glu1768 of Na<sub>v</sub>1.7-M11 were not built due to the lack of densities.  $\beta$ 2 was docked as a rigid body due to the moderate resolution.

Structure refinement was performed using phenix.real\_space\_refine application in PHENIX (14) in real space with secondary structure and geometry restraints. Over-fitting of the overall model was monitored by refining the model in one of the two independent maps from the gold-standard refinement approach and testing the refined model against the other map (15). Statistics of the map reconstruction and model refinement can be found in *SI Appendix*, Table S2.





hNa.1.1 VSLVGGSPVTSPTVQGLLPE--VIIDKPA<sup>1</sup>TDNGTITTEMRKRRSSSFHVSMDFLEDPSQRAMSIASILTNT--VEELE-----ESRQKCPFCWYKF-----SNIFLIWD<sup>2</sup>CSFYWLKV 757  
hNa.1.2 VSLVGGSPVTLTS--AGQLLP-----EGITTE<sup>1</sup>TEIRKRRSSSFHVSMDELLEDP<sup>2</sup>TSQRAMSIASILTNT--MEELE-----ESRQKCPFCWYKF-----ANVCLIND<sup>2</sup>CKPWLKV 748  
hNa.1.3 VSLVGGSPVTSPTVQGLLPE--EGITTE<sup>1</sup>TEVRRKRLSSYQISMEMLDES<sup>2</sup>SGQRAVSIASILTNT--MEELE-----ESRQKCPFCWYKF-----ANVCLIND<sup>2</sup>CCDAMLVK 749  
hNa.1.4 LDTSQG-----EKGA<sup>1</sup>PROSSGSDSGSDA--MEELE-----EAKQKCPFWYKC-----AKVLIW<sup>2</sup>NGCAPLWKF 567  
hNa.1.5 LEHPPTDTTPFSE-----EPGG<sup>1</sup>PQMLT<sup>2</sup>SQAPCVDGE<sup>3</sup>EPGARQALSAVSVL<sup>4</sup>TA--LEELE-----ESRHKCP<sup>2</sup>PCWNL--AQRYLIW<sup>2</sup>NGCAPLWMSI 706  
hNa.1.6 VSLVGGSPVTHIG--GRLLP-----EATTE<sup>1</sup>VEIKKGGGSLVSM<sup>2</sup>DQLASVYGRDRIS<sup>3</sup>MSVVT<sup>4</sup>NTLVEELE-----ESRQKCPFCWYKF-----ANTFLI<sup>2</sup>WNGHPIWKL 742  
hNa.1.7 VSLVDGRSALMLPQGLLPE--VIIDKATSD--DSGT<sup>1</sup>NQIHKKRCS<sup>2</sup>SYLLSE<sup>3</sup>MDLND<sup>4</sup>NLQRAMSRASILTNT--VEELE-----ESRQKCPFWYKF-----AKKFLI<sup>2</sup>WNGSPYIWK 733  
hNa.1.8 SELAPQAVDVSA-----FDAG<sup>1</sup>QKRTFLSAEYLD--EPFRA<sup>2</sup>QRMSVVSIIT<sup>3</sup>SV--LEELE-----ESEQKCP<sup>2</sup>PLTSL--SQKYLIND<sup>2</sup>CCPMWLK 654  
hNa.1.9 LEQTKRLSQN-----LSLD<sup>1</sup>HDFHED<sup>2</sup>GPLQ<sup>3</sup>RQALSAVSIIT<sup>4</sup>T--MKEQE-----KSE<sup>2</sup>PLCPGENL--ASKYLIND<sup>2</sup>CCQWLVC 566  
Na/PaS -----D<sup>1</sup>TTIEMNG<sup>2</sup>DEAVI<sup>3</sup>DNND<sup>4</sup>QA<sup>5</sup>RQSS-----DPETPA<sup>2</sup>SVTQRL-----D<sup>1</sup>FLCV<sup>2</sup>WD<sup>3</sup>CCVPIWQL 508

S0 S1 S2 S2.3 S3 S4 S4.5  
hNa.1.1 KHVNLVMDPFVDL<sup>1</sup>ATTCIVL<sup>2</sup>NLF<sup>3</sup>MAHE<sup>4</sup>YPMTE<sup>5</sup>DHFN<sup>6</sup>NVL<sup>7</sup>TGN<sup>8</sup>LV<sup>9</sup>FTG<sup>10</sup>FTAEM<sup>11</sup>LKI<sup>12</sup>IAMD<sup>13</sup>PIY<sup>14</sup>YQ<sup>15</sup>EG<sup>16</sup>GN<sup>17</sup>FD<sup>18</sup>GFIV<sup>19</sup>LSL<sup>20</sup>VELG--LANVEGLSV<sup>21</sup>RS<sup>22</sup>FR<sup>23</sup>LV<sup>24</sup>SV<sup>25</sup>GLA<sup>26</sup>SWPT<sup>27</sup>LNM<sup>28</sup>LI 880  
hNa.1.2 KHLVNLVMDPFVDL<sup>1</sup>ATTCIVL<sup>2</sup>NLF<sup>3</sup>MAHE<sup>4</sup>YPMTE<sup>5</sup>QFSS<sup>6</sup>VL<sup>7</sup>SVGN<sup>8</sup>LV<sup>9</sup>FTG<sup>10</sup>FTAEM<sup>11</sup>LKI<sup>12</sup>IAMD<sup>13</sup>PIY<sup>14</sup>YQ<sup>15</sup>EG<sup>16</sup>GN<sup>17</sup>FD<sup>18</sup>GFIV<sup>19</sup>LSL<sup>20</sup>VELG--LANVEGLSV<sup>21</sup>RS<sup>22</sup>FR<sup>23</sup>LV<sup>24</sup>SV<sup>25</sup>GLA<sup>26</sup>SWPT<sup>27</sup>LNM<sup>28</sup>LI 871  
hNa.1.3 KHLVNLVMDPFVDL<sup>1</sup>ATTCIVL<sup>2</sup>NLF<sup>3</sup>MAHE<sup>4</sup>YPMTE<sup>5</sup>QFSS<sup>6</sup>VL<sup>7</sup>TVGN<sup>8</sup>LV<sup>9</sup>FTG<sup>10</sup>FTAEM<sup>11</sup>LKI<sup>12</sup>IAMD<sup>13</sup>PIY<sup>14</sup>YQ<sup>15</sup>EG<sup>16</sup>GN<sup>17</sup>FD<sup>18</sup>GFIV<sup>19</sup>LSL<sup>20</sup>VELG--LSNVEGLSV<sup>21</sup>RS<sup>22</sup>FR<sup>23</sup>LV<sup>24</sup>SV<sup>25</sup>GLA<sup>26</sup>SWPT<sup>27</sup>LNM<sup>28</sup>LI 872  
hNa.1.4 KNIHLVMDPFVDL<sup>1</sup>ATTCIVL<sup>2</sup>NLF<sup>3</sup>MAHE<sup>4</sup>YPMTE<sup>5</sup>EHFN<sup>6</sup>NVL<sup>7</sup>TGN<sup>8</sup>LV<sup>9</sup>FTG<sup>10</sup>FTAEM<sup>11</sup>LKI<sup>12</sup>IAMD<sup>13</sup>PIY<sup>14</sup>YQ<sup>15</sup>EG<sup>16</sup>GN<sup>17</sup>FD<sup>18</sup>GFIV<sup>19</sup>LSL<sup>20</sup>VELG--LANVQGLSV<sup>21</sup>RS<sup>22</sup>FR<sup>23</sup>LV<sup>24</sup>SV<sup>25</sup>GLA<sup>26</sup>SWPT<sup>27</sup>LNM<sup>28</sup>LI 690  
hNa.1.5 KQGVKLVMDPFDT<sup>1</sup>ITMCI<sup>2</sup>VL<sup>3</sup>NLF<sup>4</sup>MALE<sup>5</sup>HYNM<sup>6</sup>TESE<sup>7</sup>FKN<sup>8</sup>LV<sup>9</sup>QGN<sup>10</sup>LV<sup>11</sup>FTG<sup>12</sup>FTAEM<sup>13</sup>LKI<sup>14</sup>IAMD<sup>15</sup>PIY<sup>16</sup>YQ<sup>17</sup>EG<sup>18</sup>GN<sup>19</sup>FD<sup>20</sup>GFIV<sup>21</sup>LSL<sup>22</sup>VELG--LSRMSNL<sup>23</sup>SV<sup>24</sup>RS<sup>25</sup>FR<sup>26</sup>LV<sup>27</sup>SV<sup>28</sup>GLA<sup>29</sup>SWPT<sup>30</sup>LNM<sup>31</sup>LI 829  
hNa.1.6 KEIVNLVMDPFVDL<sup>1</sup>ATTCIVL<sup>2</sup>NLF<sup>3</sup>MAHE<sup>4</sup>HPMT<sup>5</sup>PE<sup>6</sup>FHV<sup>7</sup>LAV<sup>8</sup>GN<sup>9</sup>LV<sup>10</sup>FTG<sup>11</sup>FTAEM<sup>12</sup>LKI<sup>13</sup>IAMD<sup>14</sup>PIY<sup>15</sup>YQ<sup>16</sup>EG<sup>17</sup>GN<sup>18</sup>FD<sup>19</sup>GFIV<sup>20</sup>LSL<sup>21</sup>VELG--LADVEGLSV<sup>22</sup>RS<sup>23</sup>FR<sup>24</sup>LV<sup>25</sup>SV<sup>26</sup>GLA<sup>27</sup>SWPT<sup>28</sup>LNM<sup>29</sup>LI 865  
hNa.1.7 KKCIYFVMDPFVDL<sup>1</sup>ATTCIVL<sup>2</sup>NLF<sup>3</sup>MAHE<sup>4</sup>HPMT<sup>5</sup>EE<sup>6</sup>FKN<sup>7</sup>VLA<sup>8</sup>GN<sup>9</sup>LV<sup>10</sup>FTG<sup>11</sup>FTAEM<sup>12</sup>LKI<sup>13</sup>IAMD<sup>14</sup>PIY<sup>15</sup>YQ<sup>16</sup>EG<sup>17</sup>GN<sup>18</sup>FD<sup>19</sup>GFIV<sup>20</sup>LSL<sup>21</sup>VELF--LADVEGLSV<sup>22</sup>RS<sup>23</sup>FR<sup>24</sup>LV<sup>25</sup>SV<sup>26</sup>GLA<sup>27</sup>SWPT<sup>28</sup>LNM<sup>29</sup>LI 856  
hNa.1.8 KTIILFGLVTFPAEL<sup>1</sup>ITL<sup>2</sup>CI<sup>3</sup>VN<sup>4</sup>TF<sup>5</sup>MAHE<sup>6</sup>HGM<sup>7</sup>SP<sup>8</sup>TE<sup>9</sup>FA<sup>10</sup>ML<sup>11</sup>Q<sup>12</sup>IGN<sup>13</sup>IV<sup>14</sup>TF<sup>15</sup>FTAEM<sup>16</sup>LKI<sup>17</sup>IAMD<sup>18</sup>PIY<sup>19</sup>YQ<sup>20</sup>K<sup>21</sup>KN<sup>22</sup>IFD<sup>23</sup>CLIV<sup>24</sup>TV<sup>25</sup>LSL<sup>26</sup>ELG--VAKRGLSV<sup>27</sup>RS<sup>28</sup>FR<sup>29</sup>LV<sup>30</sup>SV<sup>31</sup>GLA<sup>32</sup>SWPT<sup>33</sup>LNM<sup>34</sup>LI 777  
hNa.1.9 KRVLRVMTDPTTE<sup>1</sup>LAIT<sup>2</sup>ICII<sup>3</sup>TV<sup>4</sup>FLAME<sup>5</sup>HKME<sup>6</sup>AS<sup>7</sup>PER<sup>8</sup>KML<sup>9</sup>IGN<sup>10</sup>LV<sup>11</sup>TF<sup>12</sup>FTAEM<sup>13</sup>CLKI<sup>14</sup>IAMD<sup>15</sup>PIY<sup>16</sup>YQ<sup>17</sup>FR<sup>18</sup>GN<sup>19</sup>FD<sup>20</sup>SV<sup>21</sup>LSL<sup>22</sup>VELG--SQKYLIND<sup>23</sup>CCPMWLK 631  
Na/PaS QGAI<sup>1</sup>GA<sup>2</sup>V<sup>3</sup>LV<sup>4</sup>SP<sup>5</sup>FF<sup>6</sup>EL<sup>7</sup>LA<sup>8</sup>V<sup>9</sup>IL<sup>10</sup>IT<sup>11</sup>EMAL<sup>12</sup>DH<sup>13</sup>DM<sup>14</sup>NI<sup>15</sup>TE<sup>16</sup>FER<sup>17</sup>LR<sup>18</sup>LN<sup>19</sup>Y<sup>20</sup>TS<sup>21</sup>Y<sup>22</sup>IV<sup>23</sup>VE<sup>24</sup>AV<sup>25</sup>LK<sup>26</sup>IAL<sup>27</sup>SP<sup>28</sup>K<sup>29</sup>Y<sup>30</sup>FK<sup>31</sup>DS<sup>32</sup>N<sup>33</sup>V<sup>34</sup>DF<sup>35</sup>LV<sup>36</sup>VE<sup>37</sup>AL<sup>38</sup>ELG--LEGV<sup>39</sup>GL<sup>40</sup>SV<sup>41</sup>RS<sup>42</sup>FR<sup>43</sup>LV<sup>44</sup>SV<sup>45</sup>GLA<sup>46</sup>SWPT<sup>47</sup>LNM<sup>48</sup>LI 631

S5 P1 P2 S6  
hNa.1.1 KII<sup>1</sup>GN<sup>2</sup>SV<sup>3</sup>GAL<sup>4</sup>GN<sup>5</sup>LTV<sup>6</sup>LVA<sup>7</sup>IV<sup>8</sup>IFAV<sup>9</sup>VGM<sup>10</sup>Q<sup>11</sup>LF<sup>12</sup>G<sup>13</sup>KS<sup>14</sup>Y<sup>15</sup>K<sup>16</sup>DC<sup>17</sup>V<sup>18</sup>CK-----KI<sup>19</sup>AS<sup>20</sup>DC<sup>21</sup>QL<sup>22</sup>PR<sup>23</sup>WH<sup>24</sup>ND<sup>25</sup>DF<sup>26</sup>FS<sup>27</sup>FL<sup>28</sup>IV<sup>29</sup>FR<sup>30</sup>LV<sup>31</sup>CG<sup>32</sup>SW<sup>33</sup>LET<sup>34</sup>M<sup>35</sup>WD<sup>36</sup>C<sup>37</sup>ME<sup>38</sup>V<sup>39</sup>AG--QAM<sup>40</sup>CL<sup>41</sup>TV<sup>42</sup>FM<sup>43</sup>VM<sup>44</sup>V<sup>45</sup>GN<sup>46</sup>LV<sup>47</sup>LN<sup>48</sup>FL<sup>49</sup>LA<sup>50</sup>LL<sup>51</sup>SS<sup>52</sup>FS<sup>53</sup>A 997  
hNa.1.2 KII<sup>1</sup>GN<sup>2</sup>SV<sup>3</sup>GAL<sup>4</sup>GN<sup>5</sup>LTV<sup>6</sup>LVA<sup>7</sup>IV<sup>8</sup>IFAV<sup>9</sup>VGM<sup>10</sup>Q<sup>11</sup>LF<sup>12</sup>G<sup>13</sup>KS<sup>14</sup>Y<sup>15</sup>K<sup>16</sup>DC<sup>17</sup>V<sup>18</sup>CK-----KI<sup>19</sup>ND<sup>20</sup>CE<sup>21</sup>LR<sup>22</sup>WH<sup>23</sup>ND<sup>24</sup>DF<sup>25</sup>FS<sup>26</sup>FL<sup>27</sup>IV<sup>28</sup>FR<sup>29</sup>LV<sup>30</sup>CG<sup>31</sup>SW<sup>32</sup>LET<sup>33</sup>M<sup>34</sup>WD<sup>35</sup>C<sup>36</sup>ME<sup>37</sup>V<sup>38</sup>AG--QT<sup>39</sup>M<sup>40</sup>CL<sup>41</sup>TV<sup>42</sup>FM<sup>43</sup>VM<sup>44</sup>V<sup>45</sup>GN<sup>46</sup>LV<sup>47</sup>LN<sup>48</sup>FL<sup>49</sup>LA<sup>50</sup>LL<sup>51</sup>SS<sup>52</sup>FS<sup>53</sup>A 988  
hNa.1.3 KII<sup>1</sup>GN<sup>2</sup>SV<sup>3</sup>GAL<sup>4</sup>GN<sup>5</sup>LTV<sup>6</sup>LVA<sup>7</sup>IV<sup>8</sup>IFAV<sup>9</sup>VGM<sup>10</sup>Q<sup>11</sup>LF<sup>12</sup>G<sup>13</sup>KS<sup>14</sup>Y<sup>15</sup>K<sup>16</sup>DC<sup>17</sup>V<sup>18</sup>CK-----KI<sup>19</sup>ND<sup>20</sup>CE<sup>21</sup>LR<sup>22</sup>WH<sup>23</sup>ND<sup>24</sup>DF<sup>25</sup>FS<sup>26</sup>FL<sup>27</sup>IV<sup>28</sup>FR<sup>29</sup>LV<sup>30</sup>CG<sup>31</sup>SW<sup>32</sup>LET<sup>33</sup>M<sup>34</sup>WD<sup>35</sup>C<sup>36</sup>ME<sup>37</sup>V<sup>38</sup>AG--QT<sup>39</sup>M<sup>40</sup>CL<sup>41</sup>TV<sup>42</sup>FM<sup>43</sup>VM<sup>44</sup>V<sup>45</sup>GN<sup>46</sup>LV<sup>47</sup>LN<sup>48</sup>FL<sup>49</sup>LA<sup>50</sup>LL<sup>51</sup>SS<sup>52</sup>FS<sup>53</sup>A 989  
hNa.1.4 KII<sup>1</sup>GN<sup>2</sup>SV<sup>3</sup>GAL<sup>4</sup>GN<sup>5</sup>LTV<sup>6</sup>LVA<sup>7</sup>IV<sup>8</sup>IFAV<sup>9</sup>VGM<sup>10</sup>Q<sup>11</sup>LF<sup>12</sup>G<sup>13</sup>KS<sup>14</sup>Y<sup>15</sup>K<sup>16</sup>DC<sup>17</sup>V<sup>18</sup>CK-----KI<sup>19</sup>AL<sup>20</sup>DC<sup>21</sup>LR<sup>22</sup>WH<sup>23</sup>ND<sup>24</sup>DF<sup>25</sup>FS<sup>26</sup>FL<sup>27</sup>IV<sup>28</sup>FR<sup>29</sup>LV<sup>30</sup>CG<sup>31</sup>SW<sup>32</sup>LET<sup>33</sup>M<sup>34</sup>WD<sup>35</sup>C<sup>36</sup>ME<sup>37</sup>V<sup>38</sup>AG--QAM<sup>39</sup>CL<sup>40</sup>TV<sup>41</sup>FM<sup>42</sup>VM<sup>43</sup>V<sup>44</sup>GN<sup>45</sup>LV<sup>46</sup>LN<sup>47</sup>FL<sup>48</sup>LA<sup>49</sup>LL<sup>50</sup>SS<sup>51</sup>FS<sup>52</sup>A 807  
hNa.1.5 KII<sup>1</sup>GN<sup>2</sup>SV<sup>3</sup>GAL<sup>4</sup>GN<sup>5</sup>LTV<sup>6</sup>LVA<sup>7</sup>IV<sup>8</sup>IFAV<sup>9</sup>VGM<sup>10</sup>Q<sup>11</sup>LF<sup>12</sup>G<sup>13</sup>KS<sup>14</sup>Y<sup>15</sup>SE<sup>16</sup>LRD-----SD<sup>17</sup>SG-----L<sup>18</sup>LR<sup>19</sup>WH<sup>20</sup>ND<sup>21</sup>DF<sup>22</sup>FA<sup>23</sup>FL<sup>24</sup>IF<sup>25</sup>FR<sup>26</sup>LV<sup>27</sup>CG<sup>28</sup>SW<sup>29</sup>LET<sup>30</sup>M<sup>31</sup>WD<sup>32</sup>C<sup>33</sup>ME<sup>34</sup>VS--GQ<sup>35</sup>SL<sup>36</sup>CL<sup>37</sup>LV<sup>38</sup>FL<sup>39</sup>VM<sup>40</sup>V<sup>41</sup>GN<sup>42</sup>LV<sup>43</sup>LN<sup>44</sup>FL<sup>45</sup>LA<sup>46</sup>LL<sup>47</sup>SS<sup>48</sup>FS<sup>49</sup>A 944  
hNa.1.6 KII<sup>1</sup>GN<sup>2</sup>SV<sup>3</sup>GAL<sup>4</sup>GN<sup>5</sup>LTV<sup>6</sup>LVA<sup>7</sup>IV<sup>8</sup>IFAV<sup>9</sup>VGM<sup>10</sup>Q<sup>11</sup>LF<sup>12</sup>G<sup>13</sup>KS<sup>14</sup>Y<sup>15</sup>K<sup>16</sup>DC<sup>17</sup>V<sup>18</sup>CK-----KI<sup>19</sup>ND<sup>20</sup>CE<sup>21</sup>LR<sup>22</sup>WH<sup>23</sup>ND<sup>24</sup>DF<sup>25</sup>FS<sup>26</sup>FL<sup>27</sup>IV<sup>28</sup>FR<sup>29</sup>LV<sup>30</sup>CG<sup>31</sup>SW<sup>32</sup>LET<sup>33</sup>M<sup>34</sup>WD<sup>35</sup>C<sup>36</sup>ME<sup>37</sup>V<sup>38</sup>AG--QAM<sup>39</sup>CL<sup>40</sup>TV<sup>41</sup>FM<sup>42</sup>VM<sup>43</sup>V<sup>44</sup>GN<sup>45</sup>LV<sup>46</sup>LN<sup>47</sup>FL<sup>48</sup>LA<sup>49</sup>LL<sup>50</sup>SS<sup>51</sup>FS<sup>52</sup>A 982  
hNa.1.7 KII<sup>1</sup>GN<sup>2</sup>SV<sup>3</sup>GAL<sup>4</sup>GN<sup>5</sup>LTV<sup>6</sup>LVA<sup>7</sup>IV<sup>8</sup>IFAV<sup>9</sup>VGM<sup>10</sup>Q<sup>11</sup>LF<sup>12</sup>G<sup>13</sup>KS<sup>14</sup>Y<sup>15</sup>K<sup>16</sup>DC<sup>17</sup>V<sup>18</sup>CK-----KI<sup>19</sup>ND<sup>20</sup>CE<sup>21</sup>LR<sup>22</sup>WH<sup>23</sup>ND<sup>24</sup>DF<sup>25</sup>FS<sup>26</sup>FL<sup>27</sup>IV<sup>28</sup>FR<sup>29</sup>LV<sup>30</sup>CG<sup>31</sup>SW<sup>32</sup>LET<sup>33</sup>M<sup>34</sup>WD<sup>35</sup>C<sup>36</sup>ME<sup>37</sup>V<sup>38</sup>AG--QAM<sup>39</sup>CL<sup>40</sup>TV<sup>41</sup>FM<sup>42</sup>VM<sup>43</sup>V<sup>44</sup>GN<sup>45</sup>LV<sup>46</sup>LN<sup>47</sup>FL<sup>48</sup>LA<sup>49</sup>LL<sup>50</sup>SS<sup>51</sup>FS<sup>52</sup>A 973  
hNa.1.8 KII<sup>1</sup>GN<sup>2</sup>SV<sup>3</sup>GAL<sup>4</sup>GN<sup>5</sup>LTV<sup>6</sup>LVA<sup>7</sup>IV<sup>8</sup>IFAV<sup>9</sup>VGM<sup>10</sup>Q<sup>11</sup>LF<sup>12</sup>G<sup>13</sup>KS<sup>14</sup>Y<sup>15</sup>K<sup>16</sup>DC<sup>17</sup>V<sup>18</sup>CK-----NI<sup>19</sup>SA<sup>20</sup>PH<sup>21</sup>E--D<sup>22</sup>WR<sup>23</sup>WH<sup>24</sup>ND<sup>25</sup>DF<sup>26</sup>FS<sup>27</sup>FL<sup>28</sup>IV<sup>29</sup>FR<sup>30</sup>LV<sup>31</sup>CG<sup>32</sup>SW<sup>33</sup>LET<sup>34</sup>M<sup>35</sup>WD<sup>36</sup>C<sup>37</sup>ME<sup>38</sup>V<sup>39</sup>AG--QK<sup>40</sup>SI<sup>41</sup>CL<sup>42</sup>LV<sup>43</sup>FL<sup>44</sup>VM<sup>45</sup>V<sup>46</sup>GN<sup>47</sup>LV<sup>48</sup>LN<sup>49</sup>FL<sup>50</sup>LA<sup>51</sup>LL<sup>52</sup>SS<sup>53</sup>FS<sup>54</sup>A 895  
hNa.1.9 KII<sup>1</sup>GN<sup>2</sup>SV<sup>3</sup>GAL<sup>4</sup>GN<sup>5</sup>LTV<sup>6</sup>LVA<sup>7</sup>IV<sup>8</sup>IFAV<sup>9</sup>VGM<sup>10</sup>Q<sup>11</sup>LF<sup>12</sup>G<sup>13</sup>RS<sup>14</sup>FN<sup>15</sup>S<sup>16</sup>Q<sup>17</sup>SK<sup>18</sup>S<sup>19</sup>PK<sup>20</sup>LN<sup>21</sup>PT<sup>22</sup>GT<sup>23</sup>YS<sup>24</sup>CL<sup>25</sup>R<sup>26</sup>WH<sup>27</sup>MG<sup>28</sup>DF<sup>29</sup>HS<sup>30</sup>FL<sup>31</sup>IV<sup>32</sup>FR<sup>33</sup>LV<sup>34</sup>FR<sup>35</sup>LV<sup>36</sup>FR<sup>37</sup>LV<sup>38</sup>CG<sup>39</sup>SW<sup>40</sup>LET<sup>41</sup>M<sup>42</sup>WD<sup>43</sup>C<sup>44</sup>ME<sup>45</sup>V<sup>46</sup>AG--D<sup>47</sup>W<sup>48</sup>SC<sup>49</sup>IF<sup>50</sup>FF<sup>51</sup>AV<sup>52</sup>FG<sup>53</sup>V<sup>54</sup>GN<sup>55</sup>LV<sup>56</sup>LN<sup>57</sup>LL<sup>58</sup>LA<sup>59</sup>LL<sup>60</sup>SS<sup>61</sup>FS<sup>62</sup>A 816  
Na/PaS SVM<sup>1</sup>TK<sup>2</sup>SV<sup>3</sup>GA<sup>4</sup>V<sup>5</sup>NN<sup>6</sup>Y<sup>7</sup>M<sup>8</sup>FL<sup>9</sup>LL<sup>10</sup>EL<sup>11</sup>FA<sup>12</sup>I<sup>13</sup>GM<sup>14</sup>LF<sup>15</sup>GM<sup>16</sup>NY<sup>17</sup>DN<sup>18</sup>ME-----R<sup>19</sup>FP--D<sup>20</sup>GL<sup>21</sup>PR<sup>22</sup>WN<sup>23</sup>DF<sup>24</sup>LE<sup>25</sup>SE<sup>26</sup>MI<sup>27</sup>VER<sup>28</sup>AL<sup>29</sup>CG<sup>30</sup>EW<sup>31</sup>ES<sup>32</sup>M<sup>33</sup>WD<sup>34</sup>CL<sup>35</sup>V<sup>36</sup>AG--D<sup>37</sup>W<sup>38</sup>SC<sup>39</sup>IF<sup>40</sup>FF<sup>41</sup>AV<sup>42</sup>FG<sup>43</sup>V<sup>44</sup>GN<sup>45</sup>LV<sup>46</sup>LN<sup>47</sup>LL<sup>48</sup>LA<sup>49</sup>LL<sup>50</sup>SS<sup>51</sup>FS<sup>52</sup>A 746

hNa.1.1 DNLAA<sup>1</sup>TDD--DNEM<sup>2</sup>NLI<sup>3</sup>QI<sup>4</sup>AV<sup>5</sup>DR<sup>6</sup>M<sup>7</sup>H<sup>8</sup>GV<sup>9</sup>Y<sup>10</sup>V<sup>11</sup>RR<sup>12</sup>KI<sup>13</sup>Y<sup>14</sup>E<sup>15</sup>FI<sup>16</sup>Q<sup>17</sup>S<sup>18</sup>FI<sup>19</sup>RK--Q<sup>20</sup>KIL<sup>21</sup>DE<sup>22</sup>K<sup>23</sup>PL<sup>24</sup>DDL-----NN<sup>25</sup>K<sup>26</sup>DC<sup>27</sup>SN<sup>28</sup>HT--AE<sup>29</sup>IG<sup>30</sup>K<sup>31</sup>DL<sup>32</sup>D<sup>33</sup>YL<sup>34</sup>K<sup>35</sup>D<sup>36</sup>V<sup>37</sup>NG<sup>38</sup>T<sup>39</sup>SG<sup>40</sup>IG<sup>41</sup>T<sup>42</sup>GS<sup>43</sup>SV<sup>44</sup>E-----KY<sup>45</sup>I<sup>46</sup>DES----- 1100  
hNa.1.2 DNLAA<sup>1</sup>TDD--DNEM<sup>2</sup>NLI<sup>3</sup>QI<sup>4</sup>AV<sup>5</sup>DR<sup>6</sup>M<sup>7</sup>H<sup>8</sup>GV<sup>9</sup>Y<sup>10</sup>V<sup>11</sup>RR<sup>12</sup>KI<sup>13</sup>Y<sup>14</sup>E<sup>15</sup>FI<sup>16</sup>Q<sup>17</sup>S<sup>18</sup>FI<sup>19</sup>RK--Q<sup>20</sup>KAL<sup>21</sup>DE<sup>22</sup>K<sup>23</sup>PL<sup>24</sup>DDL-----NN<sup>25</sup>K<sup>26</sup>DC<sup>27</sup>SN<sup>28</sup>HT--IE<sup>29</sup>IG<sup>30</sup>K<sup>31</sup>DL<sup>32</sup>D<sup>33</sup>YL<sup>34</sup>K<sup>35</sup>D<sup>36</sup>V<sup>37</sup>NG<sup>38</sup>T<sup>39</sup>SG<sup>40</sup>IG<sup>41</sup>T<sup>42</sup>GS<sup>43</sup>SV<sup>44</sup>E-----KY<sup>45</sup>V<sup>46</sup>DES----- 1090  
hNa.1.3 DNLAA<sup>1</sup>TDD--DNEM<sup>2</sup>NLI<sup>3</sup>QI<sup>4</sup>AV<sup>5</sup>DR<sup>6</sup>M<sup>7</sup>H<sup>8</sup>GV<sup>9</sup>Y<sup>10</sup>V<sup>11</sup>RR<sup>12</sup>KI<sup>13</sup>Y<sup>14</sup>E<sup>15</sup>FI<sup>16</sup>Q<sup>17</sup>S<sup>18</sup>FI<sup>19</sup>RK--P<sup>20</sup>KV<sup>21</sup>IE<sup>22</sup>IE-----GN<sup>23</sup>K<sup>24</sup>DC<sup>25</sup>SN<sup>26</sup>HT<sup>27</sup>IE<sup>28</sup>IG<sup>29</sup>K<sup>30</sup>DL<sup>31</sup>D<sup>32</sup>YL<sup>33</sup>K<sup>34</sup>D<sup>35</sup>V<sup>36</sup>NG<sup>37</sup>T<sup>38</sup>SG<sup>39</sup>IG<sup>40</sup>T<sup>41</sup>GS<sup>42</sup>SV<sup>43</sup>E-----KY<sup>44</sup>V<sup>45</sup>DEN----- 1088  
hNa.1.4 DLSA<sup>1</sup>ASDE--DGM<sup>2</sup>NNL<sup>3</sup>QI<sup>4</sup>AI<sup>5</sup>GR<sup>6</sup>IK<sup>7</sup>L<sup>8</sup>G<sup>9</sup>IF<sup>10</sup>AK<sup>11</sup>FL<sup>12</sup>LL<sup>13</sup>GH<sup>14</sup>KL<sup>15</sup>SP--K<sup>16</sup>DI<sup>17</sup>ML<sup>18</sup>SL<sup>19</sup>GE<sup>20</sup>ADGA--GE<sup>21</sup>AGE<sup>22</sup>TAP<sup>23</sup>ED<sup>24</sup>KE<sup>25</sup>PP<sup>26</sup>ED<sup>27</sup>L<sup>28</sup>K<sup>29</sup>DN<sup>30</sup>HL<sup>31</sup>NH<sup>32</sup>MG--LAD<sup>33</sup>G--P<sup>34</sup>PS<sup>35</sup>LEL----- 909  
hNa.1.5 DNLTA<sup>1</sup>PDE--DREM<sup>2</sup>NNL<sup>3</sup>QI<sup>4</sup>AL<sup>5</sup>AR<sup>6</sup>IG<sup>7</sup>R<sup>8</sup>LR<sup>9</sup>FR<sup>10</sup>V<sup>11</sup>K<sup>12</sup>RT<sup>13</sup>WD<sup>14</sup>FC<sup>15</sup>GL<sup>16</sup>LR--P<sup>17</sup>Q<sup>18</sup>PA<sup>19</sup>AL<sup>20</sup>AA<sup>21</sup>Q<sup>22</sup>GL<sup>23</sup>PS<sup>24</sup>CI<sup>25</sup>AT<sup>26</sup>PS<sup>27</sup>PP<sup>28</sup>PE<sup>29</sup>TE<sup>30</sup>K<sup>31</sup>VE<sup>32</sup>PT<sup>33</sup>RE<sup>34</sup>TR<sup>35</sup>FE<sup>36</sup>EG<sup>37</sup>EQ<sup>38</sup>PG<sup>39</sup>QT<sup>40</sup>GP<sup>41</sup>PE<sup>42</sup>PVC--V<sup>43</sup>FI<sup>44</sup>AV<sup>45</sup>AS<sup>46</sup>DD<sup>47</sup>DD<sup>48</sup>EE<sup>49</sup>DE 1063  
hNa.1.6 DNLTA<sup>1</sup>PDE--DGM<sup>2</sup>NNL<sup>3</sup>QI<sup>4</sup>AV<sup>5</sup>TR<sup>6</sup>IK<sup>7</sup>GV<sup>8</sup>AM<sup>9</sup>TK<sup>10</sup>LV<sup>11</sup>HA<sup>12</sup>FM<sup>13</sup>Q<sup>14</sup>AH<sup>15</sup>--K--Q<sup>16</sup>RE<sup>17</sup>AD<sup>18</sup>VE<sup>19</sup>KL<sup>20</sup>DEL-----YE<sup>21</sup>K<sup>22</sup>AN<sup>23</sup>CI<sup>24</sup>AN<sup>25</sup>HT<sup>26</sup>GAD<sup>27</sup>I<sup>28</sup>HR<sup>29</sup>NG<sup>30</sup>DF<sup>31</sup>Q<sup>32</sup>KN<sup>33</sup>GT<sup>34</sup>SG<sup>35</sup>IG--SS<sup>36</sup>VE-----KY<sup>37</sup>I<sup>38</sup>DE----- 1081  
hNa.1.7 DNLTA<sup>1</sup>PE--D<sup>2</sup>PANN<sup>3</sup>LQI<sup>4</sup>AV<sup>5</sup>TR<sup>6</sup>IK<sup>7</sup>GV<sup>8</sup>AM<sup>9</sup>TK<sup>10</sup>LV<sup>11</sup>HA<sup>12</sup>FM<sup>13</sup>Q<sup>14</sup>AH<sup>15</sup>--K--P<sup>16</sup>KI<sup>17</sup>S<sup>18</sup>RE<sup>19</sup>QA<sup>20</sup>EDL-----NT<sup>21</sup>K<sup>22</sup>EN<sup>23</sup>YS<sup>24</sup>IN<sup>25</sup>HT<sup>26</sup>LA<sup>27</sup>MS<sup>28</sup>KG<sup>29</sup>HN<sup>30</sup>FL<sup>31</sup>KE--K<sup>32</sup>DI<sup>33</sup>SG<sup>34</sup>FG--K<sup>35</sup>HL<sup>36</sup>MEDS----- 1074  
hNa.1.8 DNLTA<sup>1</sup>PE--D<sup>2</sup>GVNN<sup>3</sup>LQ<sup>4</sup>VAL<sup>5</sup>ARI<sup>6</sup>Q--V--F<sup>7</sup>GH<sup>8</sup>RT<sup>9</sup>Q<sup>10</sup>AL<sup>11</sup>CS<sup>12</sup>FF<sup>13</sup>RS<sup>14</sup>CF<sup>15</sup>FP<sup>16</sup>K<sup>17</sup>AE<sup>18</sup>PE<sup>19</sup>LV<sup>20</sup>KL<sup>21</sup>LS<sup>22</sup>SS<sup>23</sup>KA<sup>24</sup>EN<sup>25</sup>HA<sup>26</sup>AN<sup>27</sup>TAR<sup>28</sup>GS<sup>29</sup>GG<sup>30</sup>LA<sup>31</sup>PR<sup>32</sup>GR<sup>33</sup>DE<sup>34</sup>HS<sup>35</sup>DF<sup>36</sup>AN<sup>37</sup>PT<sup>38</sup>V<sup>39</sup>W<sup>40</sup>VS--V<sup>41</sup>EI<sup>42</sup>AGE<sup>43</sup>SD<sup>44</sup>LD<sup>45</sup>LED<sup>46</sup>DD 1013  
hNa.1.9 EERN<sup>1</sup>NG<sup>2</sup>LEGE<sup>3</sup>ARK<sup>4</sup>K<sup>5</sup>V<sup>6</sup>GL<sup>7</sup>AL<sup>8</sup>DR<sup>9</sup>FR<sup>10</sup>RA<sup>11</sup>FC<sup>12</sup>VR<sup>13</sup>HT<sup>14</sup>LE<sup>15</sup>HC<sup>16</sup>HK<sup>17</sup>WK<sup>18</sup>QL<sup>19</sup>PQ<sup>20</sup>KE

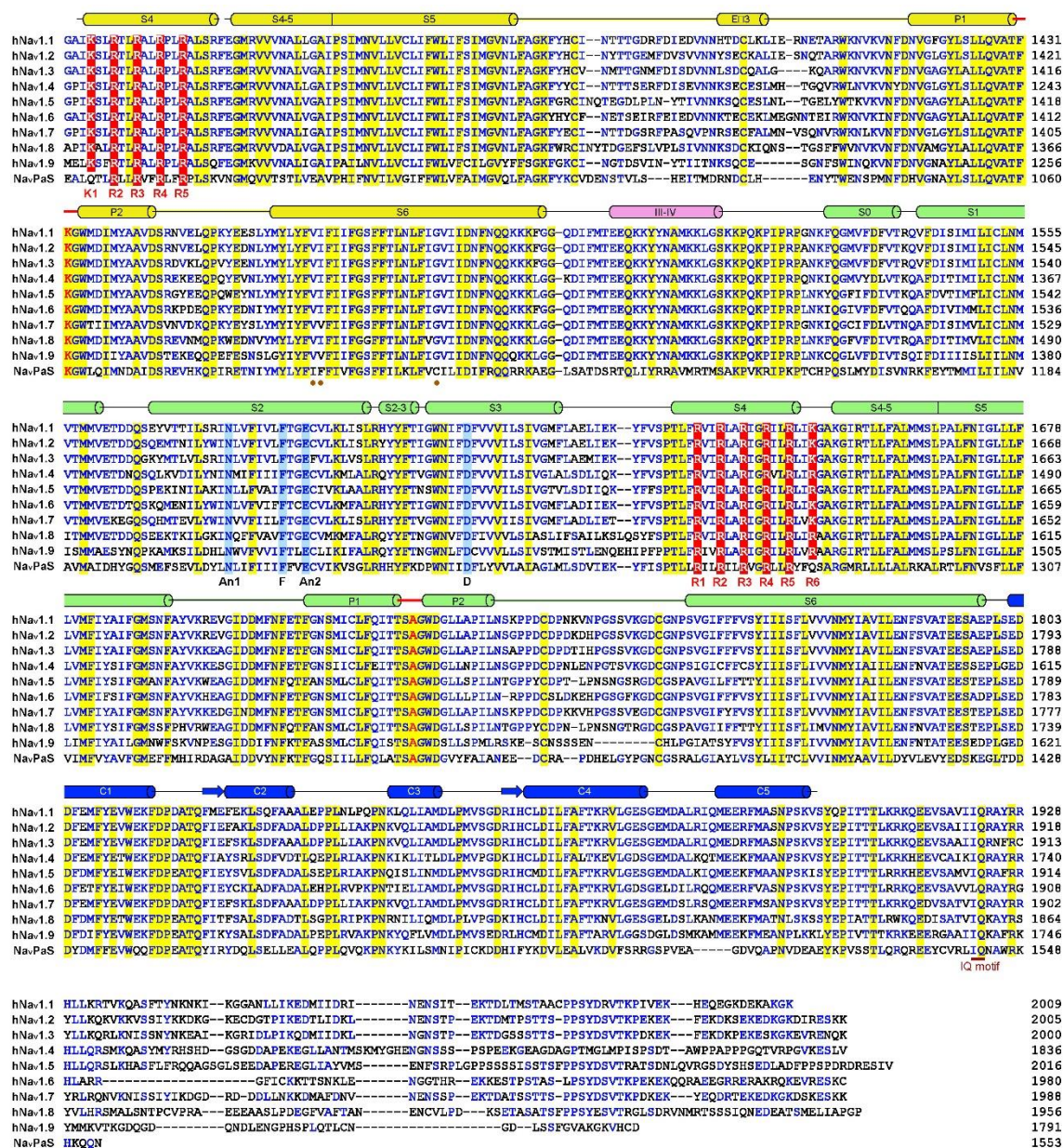


**Fig. S1 | Sequence alignment of the nine subtypes of human Na<sub>v</sub> channels and Na<sub>v</sub>-PaS.** This figure is adapted from our published sequence alignment with modifications. The sequences are aligned using Clustal W (16). Secondary structural elements of the human Na<sub>v</sub>1.7 are indicated above the sequence alignment and color-coded for the four repeats. Invariant amino acids are shaded yellow and conserved residues are colored blue. The selectivity filter motif Asp/Glu/Lys/Ala (DEKA) residues are colored red. The gating charge residues (labeled R/K1-6) in the S4 segment of each repeat are

colored white and shaded red. The residues on S2, An1, F/Y, and An2, have been reported to facilitate charge transfer. The “WQΦΦD” motif on S3 stabilizes gating charge residues in the deactivated VSD as seen in Fig. 2E. Φ stands for hydrophobic residues. The residues in Nav1.7 that are mutated to generate M11 are indicated with brown dots under the sequences. The Uniprot IDs for the aligned human Nav sequences are: Nav1.1: P35498; Nav1.2: Q99250; Nav1.3: Q9NY46; Nav1.4: P35499; Nav1.5: Q14524; Nav1.6: Q9UQD0; Nav1.7: Q15858; Nav1.8: Q9Y5Y9; Nav1.9: Q9UI33; NavPaS: D0E0C2.

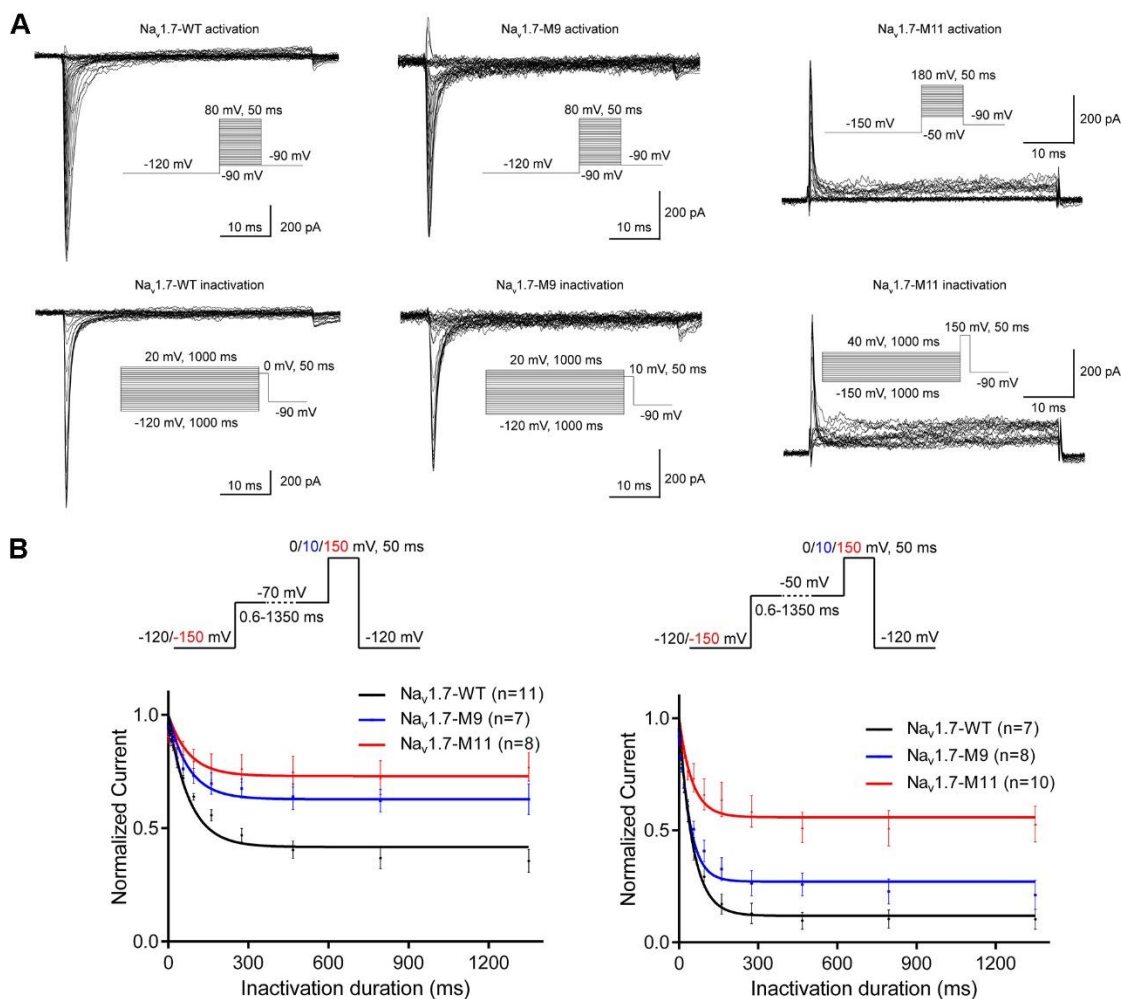


**Fig. S2 | Electrophysiological characterizations of Na<sub>v</sub>1.7 variants.** (A) Representative traces of voltage-dependent activation and inactivation for indicated Na<sub>v</sub>1.7 variants. The inset panels show the diagrams of the corresponding protocols for activation and inactivation recording. (B) Closed-state inactivation (CSI) of Na<sub>v</sub>1.7 variants. Shown here are the time courses for the development of CSI at -70 mV (*left*) and -50 mV (*right*) for the peak currents of Na<sub>v</sub>1.7 variants. The upper panels show the diagrams of the corresponding protocols. Please refer to Materials and Methods for experimental details and *SI Appendix*, Table S1 for the measured parameters.

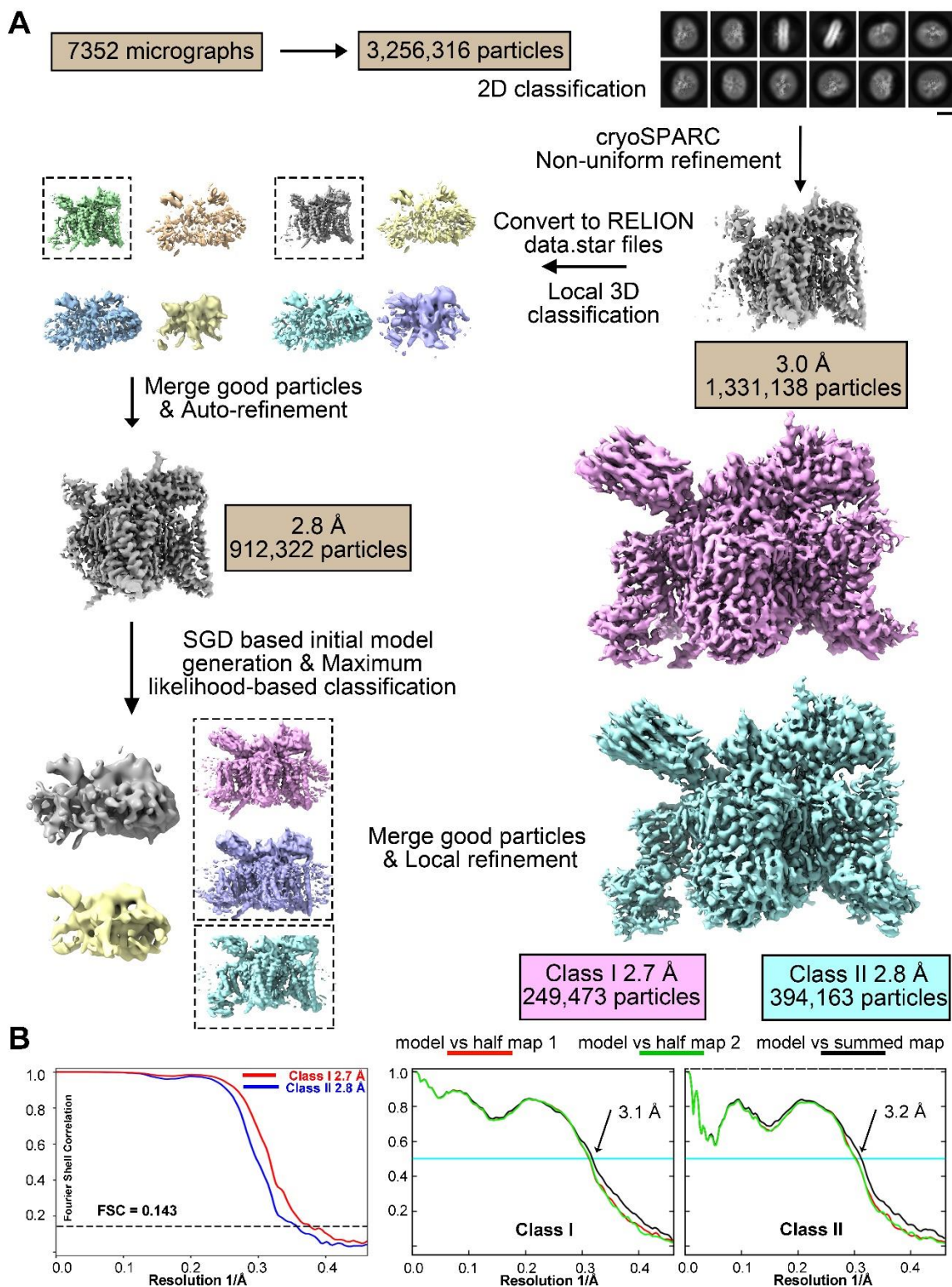


**Fig. S3 | Flowchart for EM data processing and cryo-EM analysis of Nav1.7-M11.**

(A) Flowchart for EM data processing of Nav1.7-M11. Details can be found in Materials

and Methods. The scale bar under the 2D classification represents 10 nm. (B) FSC curves. *Left*: Gold standard FSC curves for the two classes of 3D reconstructions for Na<sub>v</sub>1.7-M11. *Middle* and *right*: FSC curves of the refined models versus the overall maps that they were refined against (black), of the respective model refined in the first of the two independent maps used for the gold standard FSC versus the same map (red), and of the model refined in the first of the two independent maps versus the second independent map (green). The small difference between the red and green curves indicates that the refinement did not suffer from overfitting.

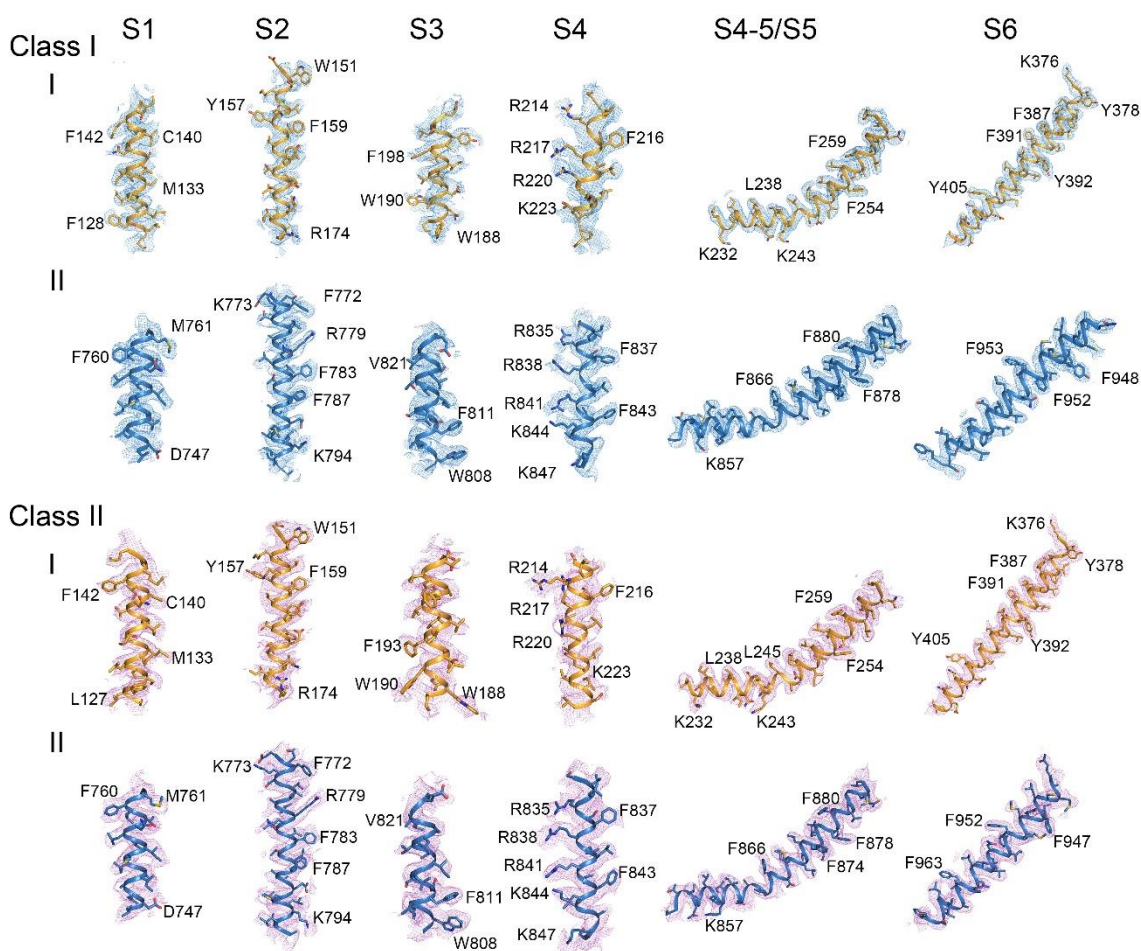


**Fig. S4 | EM maps of the segments in repeats I and II in the two classes of Na<sub>v</sub>1.7-M11.** TM segments in the first two repeats exhibit more pronounced structural shifts than repeats III and IV compared to Na<sub>v</sub>1.7-WT. The side groups of representative bulky residues that are used to validate the sequence assignment are labeled. The maps were prepared in PyMol and contoured at 4-6  $\sigma$  for S1-S4 and 8-10  $\sigma$  for S4-5, S5 and S6.

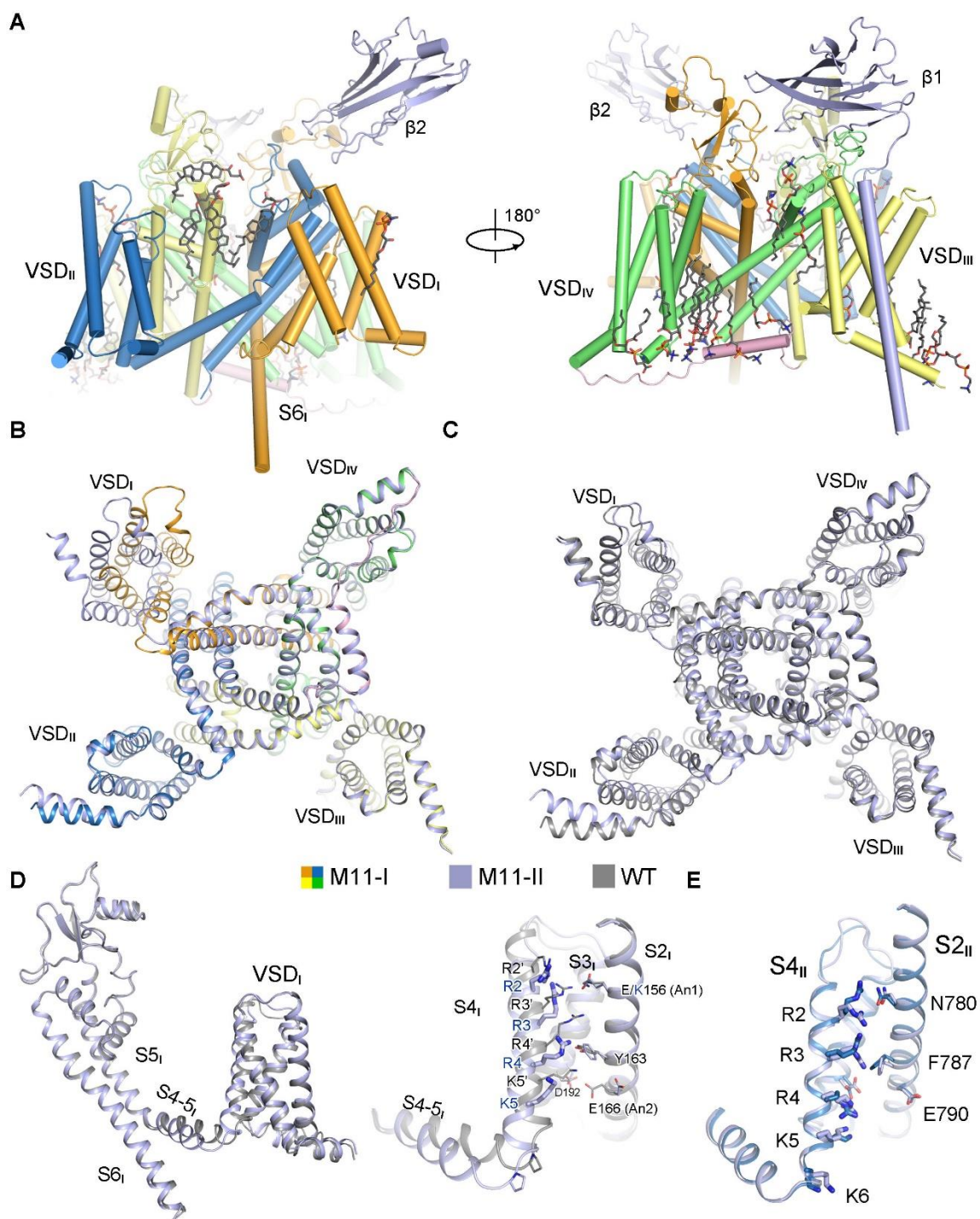


**Fig. S5 | The conformation of class II Na<sub>v</sub>.1.7-M11 is closer to that of Na<sub>v</sub>.1.7-WT despite one GC transfer in VSD<sub>I</sub> and VSD<sub>II</sub>.** (A) Overall structure of class I Na<sub>v</sub>.1.7-M11 in complex with  $\beta 1$  and  $\beta 2$ . In total 34 lipid molecules, including 8 cholesterol or cholesteryl hemisuccinate molecules, were resolved surrounding the channel. The sugar moieties are omitted. (B) The two classes of M11 mainly deviate in the position of VSD<sub>I</sub>.



Class I is domain-colored, and class II is colored pale purple. Shown here is an intracellular view of the superimposed structures. (C) The position of the VSDs in class II M11 is similar to that in WT (dark gray, PDB code: 7W9K) despite the charge transfer in VSD<sub>I</sub> and VSD<sub>II</sub>. (D) Structural deviations of VSD<sub>I</sub> and S4-5<sub>I</sub> between class II M11 and WT. *Left*: The two structures are superimposed in the context of the overall  $\alpha$  subunit. *Right*: The GC residues in VSD<sub>I</sub> of class II Na<sub>v</sub>1.7-M11 are half helical turn lower than the corresponding ones in Na<sub>v</sub>1.7-WT, while the S4-5<sub>I</sub> segment undergoes a major shift by pivoting around its C terminus. (E) Slightly different side chain orientations of R2 and R3 in VSD<sub>II</sub> of the two classes of Na<sub>v</sub>1.7-M11 structures. Otherwise, the two structures are identical in all segments other than VSD<sub>I</sub>.

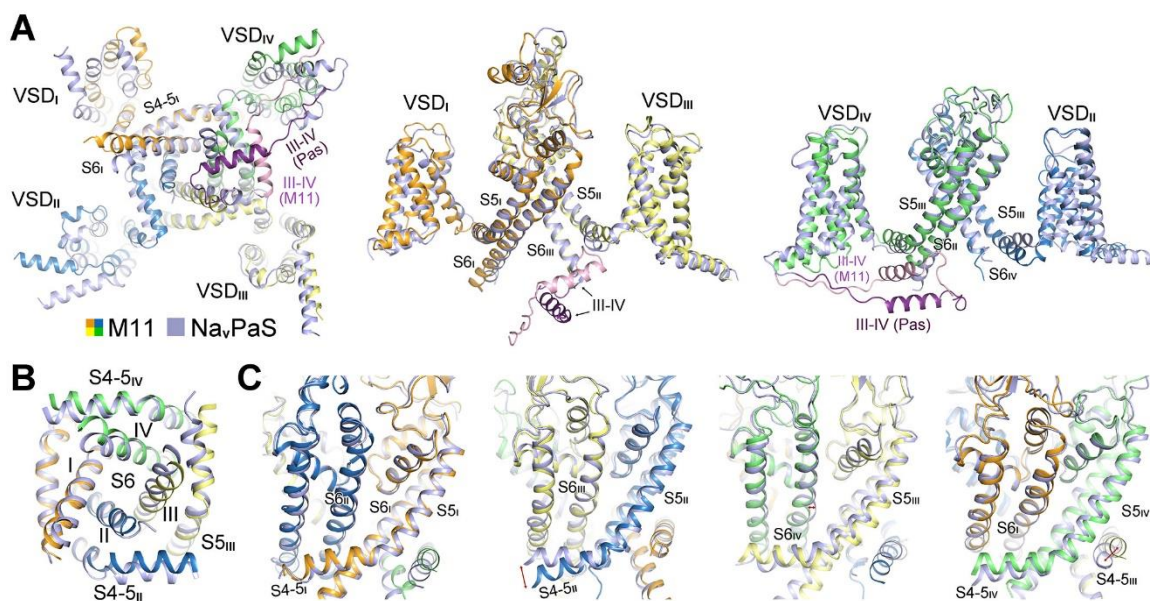


**Fig. S6 | Conformational differences between class I Na<sub>v</sub>1.7-M11 and Na<sub>v</sub>PaS. (A)**

Substantial structural deviations between Na<sub>v</sub>1.7-M11 and Na<sub>v</sub>PaS. When the two structures are superimposed relative to the PD, none of the four VSDs can be completely overlaid, an observation that is similar to the comparison between WT human Na<sub>v</sub> channels with Na<sub>v</sub>PaS. Shown on the left is an intracellular view of the superimposed α subunit of class I Na<sub>v</sub>1.7-M11 and Na<sub>v</sub>PaS, and shown on the right are the side views of superimposed diagonal repeats. (B) The intracellular gate of Na<sub>v</sub>PaS is slightly more contracted than that of Na<sub>v</sub>1.7-M11. Shown here is an enlarged intracellular view of the superimposed PD from the two channels. (C) The PD segments of Na<sub>v</sub>1.7-M11 are largely similar to those in Na<sub>v</sub>PaS except S6<sub>III</sub> and S6<sub>IV</sub>, which account for a more contracted PD in Na<sub>v</sub>PaS. The PD domains of the two channels can be superimposed with a root-mean-square deviation of ~ 1.1 Å over 440 aligned Cα atoms. Shown here are four perpendicular side views of the superimposed PD of Na<sub>v</sub>1.7-M11 and Na<sub>v</sub>PaS. Pronounced structural deviations are indicated by red double headed arrows.

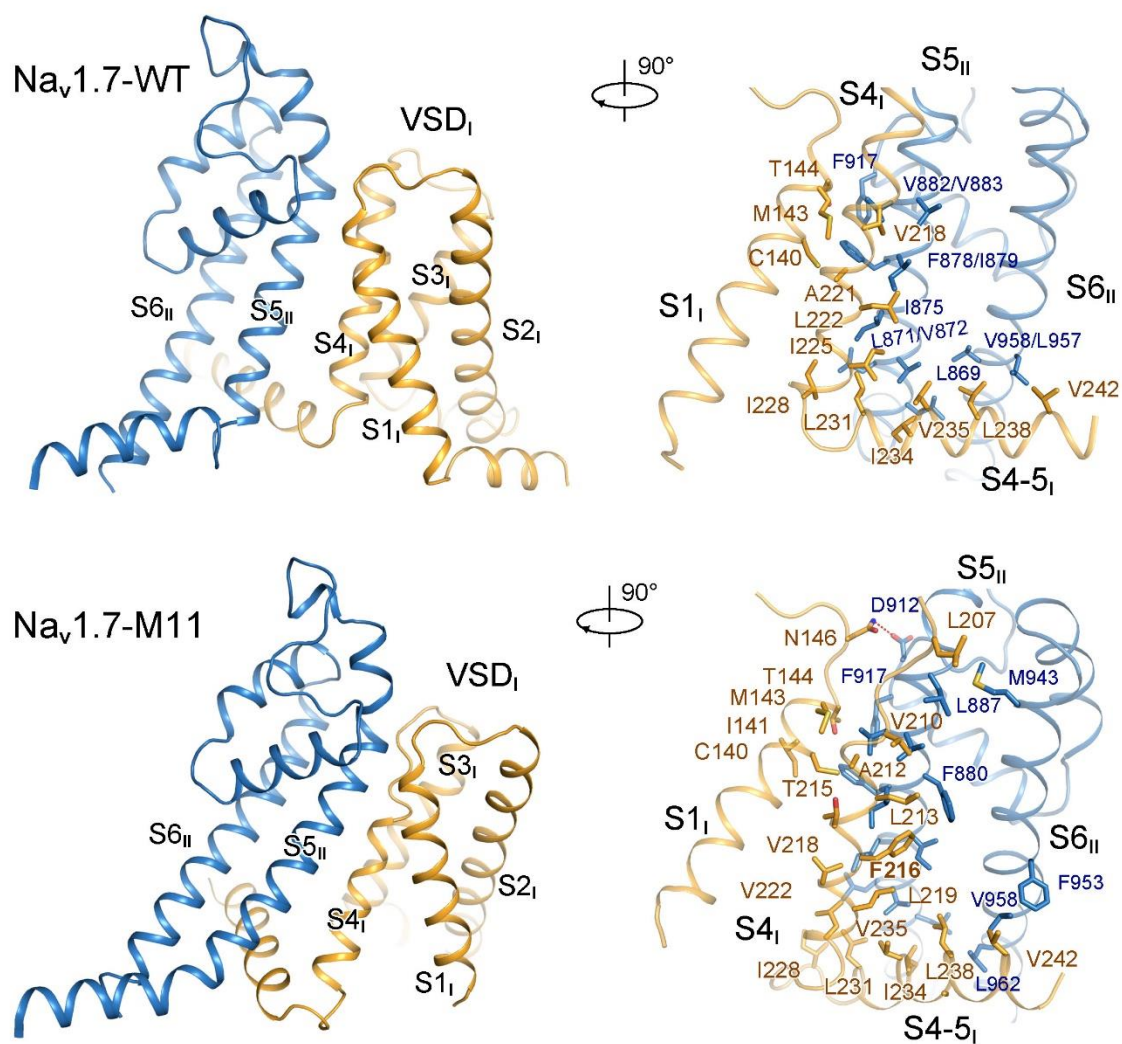


**Fig. S7 | Rearrangement of the interface between VSD<sub>I</sub> and the PD during GC transfer.** To facilitate comparison, Na<sub>v</sub>1.7-WT is also domain-colored. The residues that mediate the interaction between VSD<sub>I</sub>, S4-5<sub>I</sub>, and the pore-forming S5 and S6 segments in repeat II are shown as sticks. VSD<sub>I</sub> in the down conformation interacts more extensively with the PD of Na<sub>v</sub>1.7-M11.

**Table S1** | Activation, steady-state inactivation and closed-state inactivation parameters of Na<sub>v</sub>1.7-WT, Na<sub>v</sub>1.7-M9 and Na<sub>v</sub>1.7-M11 in HEK293T cells.

	Parameters		Na <sub>v</sub> 1.7-WT	Na <sub>v</sub> 1.7-M9	Na <sub>v</sub> 1.7-M11
Activation	V <sub>1/2</sub> (mV)		-26.02 ± 0.24	0.55 ± 0.43****	69.85 ± 0.78****
	P		/	< 0.0001	< 0.0001
	slope		5.65 ± 0.21	8.97 ± 0.40****	22.22 ± 0.73****
	P		/	< 0.0001	< 0.0001
	n		14	10	18
Inactivation	V <sub>1/2</sub> (mV)		-69.21 ± 0.37	-60.40 ± 0.56****	-49.44 ± 0.95****
	P		/	< 0.0001	< 0.0001
	slope		9.91 ± 0.33	11.11 ± 0.52	18.71 ± 0.88****
	P		/	0.075	< 0.0001
	τ <sub>inac</sub> (ms)		1.05 ± 0.11	2.01 ± 0.46**	0.45 ± 0.06*
	P		/	0.0044	0.0471
	n		17	8	12
Closed-state inactivation	Pre-holding - 70 mV	Tau (ms)	96.60 ± 5.81	50.31 ± 18.18	16.82 ± 3.19****
		P	/	0.4965	< 0.0001
	Pre-holding - 50 mV	Tau (ms)	51.15 ± 2.67	40.39 ± 2.98*	49.55 ± 6.69
		P	/	0.0427	0.8840

\* P < 0.05 versus WT, \*\* P < 0.01 versus WT, \*\*\* P < 0.001 versus WT, \*\*\*\* P < 0.0001 versus WT. Each data point represents mean ± SEM and n is the number of experimental cells from which recordings were obtained. The extra sum-of-squares F test was used to compare the V<sub>1/2</sub> and slope factor of activation and inactivation fits. τ<sub>inac</sub> values of Na<sub>v</sub>1.7-WT and mutations were compared by using one-way ANOVA analysis. The tau values of closed-state inactivation were compared by using the extra sum-of-squares F test..

**Table S2** | Statistics for data collection and model refinement.

<b>Data collection</b>		
Voltage (kV)	300	
Magnification	81,000	
Pixel size (Å)	1.0825	
Electron dose (e <sup>-</sup> /Å <sup>2</sup> )	50	
Defocus range (μm)	-1.5~ -2.5	
Number of collected micrographs	7,352	
Number of selected micrographs	7,352	
<b>Reconstruction</b>		
Software	RELION 3.1/cryoSPARC	
Symmetry	C1	
Initial particles used	3,256,316	
	Class I	Class II
Final particles used	249,473	394,163
Resolution (Å)	2.7	2.8
FSC threshold	0.143	0.143
Map resolution range (Å)	50~2.4	50~2.4
Map sharpening B-factor (Å <sup>2</sup> )	-54.6	-46.3
<b>Refinement</b>		
Initial model used (PDB code)	7W9K	7W9K
Model resolution (Å)	3.1	3.2
FSC threshold	0.5	0.5
Model composition		
Non-hydrogen atoms	12,853	12,882
Protein residues	1,541	1,529
Ligand	42	42
B factors (Å <sup>2</sup> )		
Protein	28.20	32.76
Ligand	38.49	42.39
R.m.s deviations		
Bonds length (Å)	0.025	0.033
Bonds Angle (°)	1.400	1.950
Validation		
MolProbity score	2.68	2.95
Clashscore	18.10	18.79
Poor rotamers (%)	4.04	6.65
Ramachandran plot statistics (%)		
Preferred	94.94	93.49
Allowed	5.06	6.51
Outlier	0.00	0.00

**Table S3** | Disease-related Nav1.7 mutations mapped to the interface that is re-arranged between Nav1.7-WT and Nav1.7-M11.

Nav1.7	Location	Mutation	Disease
Ile136	S1 <sub>I</sub>	I136V (17)	PERYTHM
Pro149	S1-S2 <sub>I</sub>	P149Q	Febrile seizures
Arg185	S2-S3 <sub>I</sub>	R185H (18), Nav1.2: R188W (19)	PEPD/ISFN
Ser211	S4 <sub>I</sub>	S211P (20)	PERYTHM
Phe216	S4 <sub>I</sub>	F216S (21)	PERYTHM
Ile234	S4-5 <sub>I</sub>	I234T (22)	PERYTHM
Ser241	S4-5 <sub>I</sub>	S241T (23)	PERYTHM
Leu245	S5 <sub>I</sub>	L245V	PERYTHM
Asn395	S6 <sub>I</sub>	N395K (24), Nav1.5: N406K (25)	PERYTHM
Val400	S6 <sub>I</sub>	V400M Nav1.4: V445M (26) Nav1.5: V411M (27)	PERYTHM
Glu406	S6 <sub>I</sub>	E406K (2)	PERYTHM
Ile750	S1 <sub>II</sub>	I750V	Febrile seizures/ Dravet syndrome/ ISFN
Leu834	S4 <sub>II</sub>	L834R	PERYTHM
Ile859	S4-5 <sub>II</sub>	I859T	PERYTHM
Leu869	S5 <sub>II</sub>	L869F/H	PERYTHM
Val883	S5 <sub>II</sub>	V883G	PERYTHM
Gln886	S5 <sub>II</sub>	Q886E	PERYTHM
Leu966	S6 <sub>II</sub>	L966 <sub>missing</sub>	PERYTHM

**PEPD:** Paroxysmal extreme pain disorder; **ISFN:** Idiopathic small fiber neuropathy; **PERYTHM:** Primary erythralgia. Mutations in this table are summarized from <https://www.uniprot.org/uniprot/Q15858>

## Legends for Supplementary Movies

### Movie S1 | Conformational changes between Na<sub>v</sub>1.7-WT and Na<sub>v</sub>1.7-M11.

The morph was generated in PyMol using structures of Na<sub>v</sub>1.7-M11 and Na<sub>v</sub>1.7-WT (PDB code: 7W9K) as the first and end frames. The channel is domain colored following the same scheme as in the main figures.

### Movie S2 | Gating charge (GC) transfer in VSD<sub>I</sub> and VSD<sub>II</sub>.

The GC and charge-transfer center residues are shown as thick and thin sticks, respectively, in VSD<sub>I</sub> and VSD<sub>II</sub>. The distance between L869 and I234 is shown in Å to indicate the coupled motions of S4-5<sub>I</sub> and S5<sub>II</sub> during structural shifts between Na<sub>v</sub>1.7-M11 and Na<sub>v</sub>1.7-WT. Side chains may be distorted during conformational changes owing to the limitation of the method for morph generation in PyMol.

### Movie S3 | Electromechanical coupling of GC transfer to pore gating.

Movements of VSD<sub>I</sub>, S4-5<sub>I</sub>, and S5<sub>II</sub> together drive the motion of S6 segments, leading to a pronounced change of the intracellular gate. The distance between the C $\alpha$  atoms of Asn146 above S1<sub>I</sub> and Asp912 followed by P1<sub>II</sub> is shown in Å to indicating the pivoting point for VSD<sub>I</sub> rotation.

### Movie S4 | Disease-related mutations on the interface of VSD<sub>I</sub> and the PD.

The interface between VSD<sub>I</sub> and S5<sub>II</sub> is rearranged between Na<sub>v</sub>1.7-M11 and Na<sub>v</sub>1.7-WT. Structural comparison affords important insight into the pathogenic mechanism of a number of mutations. The disease-related residues on this interface are shown as sticks.

**Supplemental References:**

1. A. Goehring *et al.*, Screening and large-scale expression of membrane proteins in mammalian cells for structural studies. *Nat Protoc* **9**, 2574-2585 (2014).
2. H. Shen, D. Liu, K. Wu, J. Lei, N. Yan, Structures of human Nav1.7 channel in complex with auxiliary subunits and animal toxins. *Science* **363**, 1303-1308 (2019).
3. J. Lei, J. Frank, Automated acquisition of cryo-electron micrographs for single particle reconstruction on an FEI Tecnai electron microscope. *J Struct Biol* **150**, 69-80 (2005).
4. S. Q. Zheng *et al.*, MotionCor2: anisotropic correction of beam-induced motion for improved cryo-electron microscopy. *Nat Methods* **14**, 331-332 (2017).
5. T. Grant, N. Grigorieff, Measuring the optimal exposure for single particle cryo-EM using a 2.6 Å reconstruction of rotavirus VP6. *Elife* **4**, e06980 (2015).
6. K. Zhang, Gctf: Real-time CTF determination and correction. *J Struct Biol* **193**, 1-12 (2016).
7. A. Punjani, J. L. Rubinstein, D. J. Fleet, M. A. Brubaker, cryoSPARC: algorithms for rapid unsupervised cryo-EM structure determination. *Nat Methods* **14**, 290-296 (2017).
8. S. H. Scheres, RELION: implementation of a Bayesian approach to cryo-EM structure determination. *J Struct Biol* **180**, 519-530 (2012).
9. S. H. Scheres, Semi-automated selection of cryo-EM particles in RELION-1.3. *J Struct Biol* **189**, 114-122 (2015).
10. D. Kimanius, B. O. Forsberg, S. H. Scheres, E. Lindahl, Accelerated cryo-EM structure determination with parallelisation using GPUs in RELION-2. *Elife* **5** (2016).
11. D. Asarnow, E. Palovcak, Y. Cheng, UCSF pyem v0.5. Zenodo. <https://doi.org/10.5281/zenodo.3576630> (2019).
12. E. F. Pettersen *et al.*, UCSF Chimera--a visualization system for exploratory research and analysis. *J Comput Chem* **25**, 1605-1612 (2004).
13. P. Emsley, B. Lohkamp, W. G. Scott, K. Cowtan, Features and development of Coot. *Acta Crystallogr D Biol Crystallogr* **66**, 486-501 (2010).
14. P. D. Adams *et al.*, PHENIX: a comprehensive Python-based system for macromolecular structure solution. *Acta Crystallogr D Biol Crystallogr* **66**, 213-221 (2010).
15. A. Amunts *et al.*, Structure of the yeast mitochondrial large ribosomal subunit. *Science* **343**, 1485-1489 (2014).
16. M. A. Larkin *et al.*, Clustal W and Clustal X version 2.0. *Bioinformatics* **23**, 2947-2948 (2007).
17. X. Cheng, S. D. Dib-Hajj, L. Tyrrell, S. G. Waxman, Mutation I136V alters electrophysiological properties of the Na(v)1.7 channel in a family with onset of erythromelalgia in the second decade. *Mol Pain* **4**, 1 (2008).
18. C. Han *et al.*, Functional profiles of SCN9A variants in dorsal root ganglion neurons and superior cervical ganglion neurons correlate with autonomic symptoms in small fibre neuropathy. *Brain* **135**, 2613-2628 (2012).



19. T. Sugawara *et al.*, A missense mutation of the Na<sup>+</sup> channel alpha II subunit gene Na(v)1.2 in a patient with febrile and afebrile seizures causes channel dysfunction. *Proceedings of the National Academy of Sciences of the United States of America* **98**, 6384-6389 (2001).
20. M. Estacion *et al.*, Can robots patch-clamp as well as humans? Characterization of a novel sodium channel mutation. *J Physiol* **588**, 1915-1927 (2010).
21. J. S. Choi, S. D. Dib-Hajj, S. G. Waxman, Inherited erythromelgia: limb pain from an S4 charge-neutral Na channelopathy. *Neurology* **67**, 1563-1567 (2006).
22. H. S. Ahn *et al.*, A new Nav1.7 sodium channel mutation I234T in a child with severe pain. *Eur J Pain* **14**, 944-950 (2010).
23. A. Lampert, S. D. Dib-Hajj, L. Tyrrell, S. G. Waxman, Size Matters: Erythromelgia Mutation S241T in Nav1.7 Alters Channel Gating \*. *Journal of Biological Chemistry* **281**, 36029-36035 (2006).
24. P. L. Sheets, J. O. Jackson, 2nd, S. G. Waxman, S. D. Dib-Hajj, T. R. Cummins, A Nav1.7 channel mutation associated with hereditary erythromelgia contributes to neuronal hyperexcitability and displays reduced lidocaine sensitivity. *The Journal of physiology* **581**, 1019-1031 (2007).
25. R. M. Hu *et al.*, Mexiletine rescues a mixed biophysical phenotype of the cardiac sodium channel arising from the SCN5A mutation, N406K, found in LQT3 patients. *Channels (Austin)* **12**, 176-186 (2018).
26. M. P. Takahashi, S. C. Cannon, Enhanced slow inactivation by V445M: a sodium channel mutation associated with myotonia. *Biophysical journal* **76**, 861-868 (1999).
27. A. J. Horne, J. Eldstrom, S. Sanatani, D. Fedida, A novel mechanism for LQT3 with 2:1 block: a pore-lining mutation in Nav1.5 significantly affects voltage-dependence of activation. *Heart rhythm* **8**, 770-777 (2011).